Published in :Journal of Mining Science, 2017, 53(1):25-37

Strain gradient model of zonal disintegration of rock mass near deep level tunnels

Chengzhi Qi[a*], Kairui Li[a,b] , Jiping Bai[c], Anvar Chanyshev[d], Peng Liu[a]

[a]Beijing Future Urban Design High-Tech Innovation Center and 2011 Energy Conservation and Emission reduction Collaborative Innovation Center, Beijing University of Civil Engineering and Architecture, Beijing, 100044, China, e-mail: qichengzhi65@163.com

[b]Defense Engineering Institute, PLA University of Science and Technology, Nanjing, 210007, P R China

[c]Faculty of Computing, Engineering & Science, University of South Wales, Pontypridd, CF37 1DL, UK

[d]Chinakal Mining Institute, SB RAS,54 Krasny prospect, Novosibirsk, 630091,Russia;e-mail: a.i.chanyshev@gmail.com

Abstract: This paper presents one strain gradient model of zonal disintegration of rock mass near deep level tunnel. The governing equations and boundary conditions of the model are established. Numerical methods (Quasi-Newton method and Shooting method) are adopted to solve the obtained fourth-order equilibrium equations with higher-order boundary conditions in terms of displacement. The stress field in elastic and plastic zones is obtained. The effects of model parameters on stresses distribution in surrounding the tunnel rock mass are examined. The necessary conditions for the formation of zonal disintegration are elucidated.

Key words: deep-level tunnel, rock mass, zonal disintegration, strain gradient model

1. Introduction

In the 1970's and the early1980's it was found that zonal disintegration in the surrounding deep level underground tunnel rock mass occurs [1] (Fig.1). In-situ observations continued to confirm the existence of this phenomenon [2]. The feature of this phenomenon lies in the localization of fracture of rock mass in discrete zones, which alternate with relatively weakly fractured zones in the form of the contour of the tunnels.

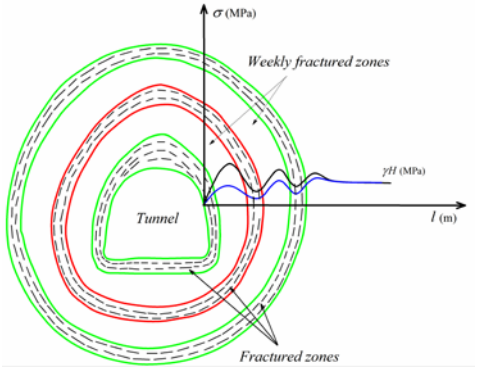

Fig.1 Zonal disintegration near deep level tunnel

It has been over three decades since the discovery of zonal disintegration, but the formation mechanism of this phenomenon is still not clear. Experimental and theoretical investigations have been systematically carried out by Shemyakin et al [3-5]. It was thought that this phenomenon is as a result of the splitting of rock mass along the direction of the maximum tangential compression stress when the lateral compression stresses are small [4]. When splitting occurs, "false" opening contour forms and the stresses in the rock mass will be redistributed. The splitting process continues until the unsatisfactory condition of splitting is reached. The experiments carried out by Kurlenja et al [6] have shown that due to non-continuity in rock mass, the deformation of rock mass does not satisfy the deformation compatibility condition of Saint-Venant, but satisfy the condition of the smallness of the

* Corresponding author. Tel.: +86 10 68322492, 13701328772 (mobile).
E-mail addresses: qichengzhi65@163.com, qichengzhi@bucea.edu.cn (C. Qi).

lateral compression. Experiments carried out by Gu et al [7] and Zhang et al [8] reproduced this phenomenon. Gu et al [7] concluded that the realization of plane strain condition is necessary for the reproduction of zonal disintegration.

Chanyshev [9, 10] studied zonal disintegration phenomenon using slip line field theory. He considered arbitrary compressibility and softening of rock mass and showed that when magnitude of softening modulus approaches to elastic bulk modulus of rock mass, one of the four developed systems of slip lines repeats the form of the contour of tunnel. This system of slip lines represents zonal disintegration phenomenon. Guzev and Paroshin [11] applied non-Euclidean geometry model to zonal disintegration phenomenon and obtained the quasi-periodic solutions of non-compatibility parameter R and stresses near deep level tunnel along radial direction. Essentially their model is elastic one with defects, no plastic deformation is involved in.

One of the important features of rock mass is its internal structure. To consider the internal structure of media many high-order theories have been proposed which incorporate gradients of appropriate physical state variables together with one or more intrinsic length scales in their constitutive formulations. Gradient theories may be divided into two distinct groups [12, 13]. The first group is the strain gradient models (for example, [14-18]). The second group includes models with gradients of internal variables, for example [19-23]. The fundamental difference between these two groups of models is that in the first group of models strain gradients considered as additional observable state variables are conjugate to higher-order stresses that enter the equilibrium equations, while gradients of internal variables are conjugate to certain dissipative thermodynamic forces that can enter the evolution equations for internal variables but do not appear in the equilibrium (momentum balance) equations.

Model with gradients of internal variable (cumulative effective plastic strain) developed by Wang, Qi et al [24] has been applied to the zonal disintegration phenomenon. For circular tunnels the quasi-periodic solution of effective plastic strain for ideal brittle rock mass is given. The shortcoming of models with gradients of internal variables is that gradient terms do not enter equilibrium equations; therefore the gradient-dependent stress-strain fields in surrounding tunnel rock mass cannot be determined in self-consistent way.

At present there is a lack of mechanical model that takes into account the plastic properties of materials and gives the quasi-periodic oscillating solutions for stresses and strains on the basis of equilibrium equations. This paper presents the work carried out recently by the authors on modeling zonal disintegration phenomenon. The general governing equations of the model are derived. The stress fields are obtained with numerical methods. The influence of model parameters on stress distribution in surrounding the tunnel rock mass is analyzed. The importance of these parameters for the formation of zonal disintegration is elucidated.

2. Principle of virtual work

Assume that the components of displacement vector $\mathbf{u}$ of rock are u_i, and the components of strain tensor $\boldsymbol{\varepsilon}$ of rock are ε_{ij}, then for small strain we have the following geometric relation:

$$\varepsilon_{ij} = \left(u_{i,j} + u_{j,i}\right)/2 \tag{1}$$

Strain tensor ε_{ij} may be decomposed into elastic part ε_{ij}^e and plastic part ε_{ij}^p:

$$\varepsilon_{ij} = \varepsilon_{ij}^e + \varepsilon_{ij}^p \tag{2}$$

To apply strain gradient theory to modeling zonal disintegration and to characterize the gradient nature of the material behavior of a continuous particle system it is assumed that there exists an internal energy potential of the following form:

$$U = U\left(\boldsymbol{\varepsilon}^e, \nabla\boldsymbol{\varepsilon}, \eta, E^p\right), \tag{3}$$

where $E^p = \sqrt{\varepsilon_{ij}^p \varepsilon_{ij}^p}$ is the cumulative effective plastic deformation; $\boldsymbol{\varepsilon}^e$ is the elastic strain tensor; $\nabla\boldsymbol{\varepsilon}$ is the gradient of total strain tensor $\boldsymbol{\varepsilon}$; η is the entropy.

The principle of virtual work states that, given any sub-body V, the virtual work expended on V by materials or bodies exterior to V (i.e. the external work) be equal to the virtual work expended within V (i.e. the internal work). External work is assumed to be done by macroscopic body force $\mathbf{F_b}$, macroscopic surface traction $\mathbf{F_s}$:

$$W_{ext} = \int_V \mathbf{F_b} \cdot \delta\mathbf{u} dV + \int_\Gamma \mathbf{F_s} \cdot \delta\mathbf{u} d\Gamma \tag{4}$$

where δ is variation parameter; $\delta\mathbf{u}$ denotes virtual displacement.

External work W_{ext} is balanced by internal work W_{int}. The internal work is assumed to arise from elastic stress tensor $\boldsymbol{\sigma}$, generalized force $\boldsymbol{\Omega}$ conjugate to plastic strain tensor ε_{ij}^p, generalized force $\mathbf{B}$ conjugate to effective plastic strain E^p, generalized force $\mathbf{T}$ conjugate to $\nabla\boldsymbol{\varepsilon}$:

$$W_{int} = \int_V \boldsymbol{\sigma} \cdot \delta\boldsymbol{\varepsilon}^e dV + \int_V \boldsymbol{\Omega} \cdot \delta\boldsymbol{\varepsilon}^p dV + \int_V \mathbf{B} \cdot \delta E^p dV + \int_V \mathbf{T} \cdot \delta\nabla\boldsymbol{\varepsilon} dV \tag{5}$$

where

$$\delta E^p = \frac{\varepsilon_{ij}^p \delta\varepsilon_{ij}^p}{\sqrt{\varepsilon_{mn}^p \varepsilon_{mn}^p}} = \frac{\varepsilon_{ij}^p \delta\varepsilon_{ij}^p}{E^p} = p_{ij}\delta\varepsilon_{ij}^p \tag{6}$$

where $p_{ij} = \varepsilon_{ij}^p \big/ E^p$ is the plastic strain orientation tensor, introduced by A.A. Iliushin [25]

The principle of virtual work may be expressed as $W_{ext} = W_{int}$, from which we obtain:

$$\begin{aligned} &\int_V \left(\sigma_{ij,j} - T_{ijk,kj} + F_{bi}\right)\delta u_i dV + \int_\Gamma \left[F_{si} - (\sigma_{ij} - T_{ijk,k})\ n_j + \kappa_i\right] n_j \delta u_i d\Gamma + \\ &\int_V \left[\left(\sigma_{ij} - \Omega_{ij} - Bp_{ij}\right)\right]\delta\varepsilon_{ij}^p dV + \int_\Gamma (T_{ijk} n_k) n_j \frac{\partial \delta u_i}{\partial n} d\Gamma = 0 \end{aligned} \tag{7}$$

where n_j is the unit normal to the surface Γ of the body, $\kappa_i = [kn_j - (\delta_{jm} - n_j n_m)\partial_m](T_{ijk} n_k)$, in the deduction of which besides Gauss's theorem, surface divergence theorem is also used [15].

Because of the arbitrariness of δu_i and $\delta\varepsilon_{ij}^p$, the following equations are obtained from Eq. (7):

$$\sigma_{ij,j} - T_{ijk,kj} + F_{bi} = 0 \tag{8}$$

$$F_{si} - (\sigma_{ij} - T_{ijk,k})\ n_j + \kappa_i = 0 \tag{9}$$

$$\sigma_{ij} - \Omega_{ij} - Bp_{ij} = 0 \tag{10}$$

$$T_{ijk} n_k n_j = 0 \tag{11}$$

Eq.(8) is the equilibrium equation of the medium, in which gradient term is included; Eq. (9) is the macroscopic boundary conditions; Eq. (10) defines the yield condition and Eq.(11) is the higher-order boundary conditions. By taking the Euclidean norm $\| \ \|$ of Eq. (10), then $\left\|\sigma_{ij} - \Omega_{ij}\right\| = B$, where Ω_{ij} represents the kinematic hardening parameter. In the case of isotropic hardening, $\Omega_{ij} = 0$, we have $\left\|\sigma_{ij}\right\| = B$. Therefore parameter B has the physical meaning of yield stress of material.

3. The basic equations of rock mass dear deep level circular tunnels in elastic regime

When body force is neglected, Eq.(8) has the form

$$\sigma_{ij,j} + T_{ijk,kj} = 0 \tag{12}$$

Within the framework of linear elasticity, the generalized Hooke's law between σ_{ij} and ε_{ij} and between τ_{ijk} and $\eta_{ijk} = u_{k,ij}$ are assumed [15, 16]

$$\sigma_{ij} = \lambda\varepsilon_{kk}\delta_{ij} + 2\mu\varepsilon_{ij};$$
$$\tau_{ijk} = l^2[a_1(\eta_{ipp}\delta_{jk} + \eta_{jpp}\delta_{ik}) + a_2(\eta_{ppi}\delta_{jk} + 2\eta_{kpp}\delta_{ij} + \eta_{ppj}\delta_{ik}) + a_3\eta_{ppk}\delta_{ij} + a_4\eta_{ijk} + a_5(\eta_{kji} + \eta_{kij})] \tag{13}$$

where λ and μ are Lamé's constants; l is the internal length scale due to the introduction of strain gradients; a_i $(i = 1,\cdots 5)$ are elastic constants associated with gradient terms in a material.

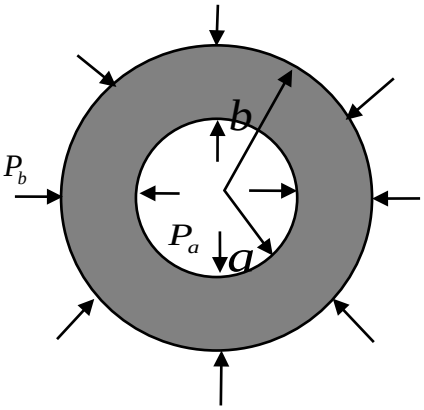

Fig.2 Model of cylinder

For axisymmetric problem of circular cylinder, shown in Fig.2, displacements u_i don't depend on θ and z coordinates, but depend only on r coordinate. Under plane strain condition only 6 components of the conventional strains ε_{ij} and strain gradients η_{ijk} [17] are non-zero: ε_r, ε_θ, η_{rrr}, $\eta_{\theta\theta r}$, $\eta_{r\theta\theta}$ and $\eta_{\theta r\theta}$, which can be expressed in terms of radial displacement u_r in the following form:

$$\varepsilon_r = u_{r,r}, \varepsilon_\theta = \frac{u_r}{r},$$
$$\eta_{rrr} = u_{r,rr}, \eta_{\theta\theta r} = \frac{1}{r^2}(ru_{r,r} - u), \eta_{r\theta\theta} = \eta_{\theta r\theta} = \frac{1}{r}(u_{r,r} - \frac{u_r}{2r}) \tag{14}$$

Eq. (12) then gives the following equilibrium equation for the radial direction:

$$\frac{\partial}{\partial r}[\sigma_r - \frac{\partial\tau_{rrr}}{\partial r} - \frac{1}{r}(\tau_{rrr} - \tau_{\theta\theta r} - \tau_{r\theta\theta})]$$
$$+\frac{1}{r}[\sigma_r - \sigma_\theta - \frac{\partial\tau_{rrr}}{\partial r} + \frac{\partial\tau_{\theta r\theta}}{\partial r} - \frac{1}{r}(\tau_{rrr} - 2\tau_{\theta\theta r} - 2\tau_{r\theta\theta} - \tau_{\theta r\theta})] = 0 \tag{15}$$

The boundary conditions of Eqs.(9) and (11) on the inner $r = a$ and outer $r = b$ radii of the cylinder take the following form, respectively

$$T_{r=a} = -\sigma_r + \frac{\partial\tau_{rrr}}{\partial r} + \frac{1}{r}(-\tau_{rrr} - \tau_{\theta\theta r}) = p_a; \quad R_{r=a} = \tau_{rrr} = 0 \tag{16}$$

$$T_{r=b} = \sigma_r - \frac{\partial\tau_{rrr}}{\partial r} + \frac{1}{r}(-\tau_{rrr} + 2\tau_{r\theta\theta} + \tau_{\theta\theta r}) = -p_b; \quad R_{r=b} = \tau_{rrr} = 0 \tag{17}$$

where $R_{r=a}$ and $R_{r=b}$ are values of high order stresses on the inner $r = a$ and outer $r = b$ radii of the cylinder.

Substituting Eq.(14) into Eq.(13) yields

$$\sigma_r = \frac{E}{(1-2\upsilon)(1+\upsilon)}[(1-\upsilon)\frac{\partial u_r}{\partial r} + \upsilon\frac{u_r}{r}]; \quad \sigma_\theta = \frac{E}{(1-2\upsilon)(1+\upsilon)}[\upsilon\frac{\partial u_r}{\partial r} + (1-\upsilon)\frac{u_r}{r}] \tag{18}$$

$$\begin{cases} \tau_{rrr}= cl^2(5\dfrac{\partial^2 u_r}{\partial r^2}+4\dfrac{\partial u_r}{r\partial r}-\dfrac{13}{4}\dfrac{u_r}{r^2}); \quad \tau_{r\theta\theta}=\tau_{\theta r\theta}= cl^2(\dfrac{3}{4}\dfrac{\partial^2 u_r}{\partial r^2}+\dfrac{11}{4}\dfrac{\partial u_r}{r\partial r}-\dfrac{7}{4}\dfrac{u_r}{r^2}) \\ \tau_{rzz}=\tau_{zrz}= cl^2(\dfrac{3}{4}\dfrac{\partial^2 u_r}{\partial r^2}+\dfrac{3}{4}\dfrac{\partial u_r}{r\partial r}-\dfrac{1}{2}\dfrac{u_r}{r^2}); \quad \tau_{\theta\theta r}= cl^2(\dfrac{3}{2}\dfrac{\partial^2 u_r}{\partial r^2}+\dfrac{7}{2}\dfrac{\partial u_r}{r\partial r}-\dfrac{11}{4}\dfrac{u_r}{r^2}) \\ \tau_{zzr}= cl^2(\dfrac{3}{2}\dfrac{\partial^2 u_r}{\partial r^2}+\dfrac{3}{2}\dfrac{\partial u_r}{r\partial r}-\dfrac{5}{4}\dfrac{u_r}{r^2}) \end{cases} \tag{19}$$

where υ is Poisson's ratio.

4. The basic equations of rock mass dear deep level circular tunnels in plastic regime

4.1 The constitutive equations in plastic regime

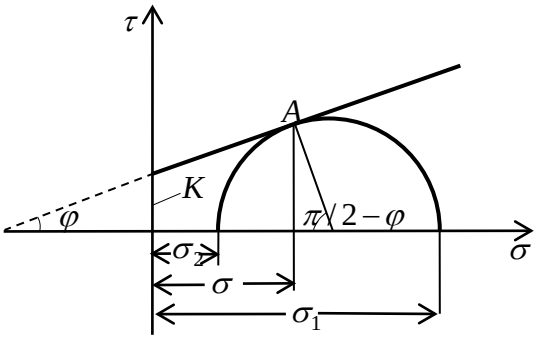

Fig.3 Envelop of Mohr's circles of principal stresses

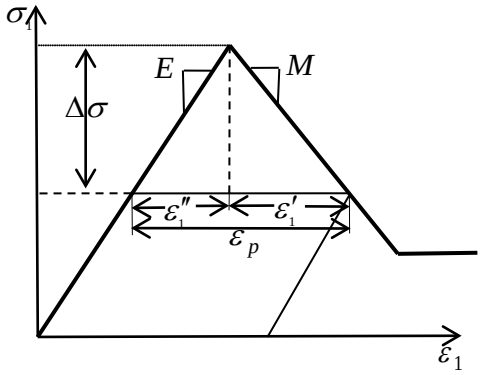

Fig.4 Stress-strain curve with softening

For geomedia Mohr-Couloumb criterion is the most popular yield criterion, with which the shear strength τ of geomedia depends on the normal stress σ on the slip surface. For the envelop of Mohr's circles of principal stresses shown in Fig.3 the Mohr-Couloumb criterion may be expressed as follows [26]

$$\tau = \sigma \cdot tan\varphi + K \tag{20}$$

where K is the internal cohesion, and φ is the friction angle. Or in principal stresses σ_1,σ_3

$$\sigma_1 - A\sigma_3 = \sigma_c \tag{21}$$

Where $A=\dfrac{1+sin\varphi}{1-sin\varphi}$, $\sigma_c=\dfrac{2K\,cos\varphi}{1-sin\varphi}$ represents the compressive strength.

For rock mass with softening (see Fig.4) the descending branch may be expressed as

$$\sigma_1 - A\sigma_3 = \sigma_c - |M|\varepsilon_1' \tag{22}$$

where $|M|$ is the softening modulus; ε_1' is the deformation increment beyond strength limit in the direction of σ_1.

By introducing lateral deformation coefficient $\beta = |\varepsilon_3'/\varepsilon_1'|$ Eq.(22) becomes

$$\sigma_1 - A\sigma_3 = \sigma_c - |M|\,\varepsilon_3'/\beta \tag{23}$$

For plane strain problem after some operations the constitutive relations can be expressed in the following form

$$\sigma_1 = k_1\varepsilon_1 + m_1\varepsilon_3 + n_1; \sigma_3 = k_2\varepsilon_1 + m_2\varepsilon_3 + n_2 \tag{24}$$

where

$$k_1=\frac{b_2}{a_1b_2-a_2b_1};m_1=\frac{-b_1}{a_1b_2-a_2b_1};n_1=\frac{b_1c_2-b_2c_1}{a_1b_2-a_2b_1}$$

$$k_2=\frac{-a_2}{a_1b_2-a_2b_1};m_2=\frac{a_1}{a_1b_2-a_2b_1};n_2=\frac{a_2c_1-a_1c_2}{a_1b_2-a_2b_1}$$

$$a_1=\frac{1-\upsilon^2}{E}-\frac{1+\xi}{|M|};b_1=\frac{1+\xi}{|M|}A-\frac{(1+\upsilon)\upsilon}{E};c_1=\frac{1+\xi}{|M|}\sigma_c;$$

$$a_2=-\frac{(1+\upsilon)\upsilon}{E}+\frac{\beta+\xi\upsilon}{|M|};b_2=-\frac{\beta+\xi\upsilon}{|M|}A+\frac{1-\upsilon^2}{E};c_2=-\frac{\beta+\xi\upsilon}{|M|}\sigma_c$$

4.2 The governing equations in elastic-plastic regime

Now let's again consider the axisymmetric plane strain problem as shown in Fig.5. The translucent circle area is the excavated tunnel with radius a, the supporting force applied on inner surface of the tunnel is p_a; the black part is the plastic zone with radius ρ; the white ring area with inner radius ρ and outer radius b is the elastic zone, on the cylindrical surface of radius b hydro-geostatic pressure p_b applies. The case when $b\to\infty$ corresponds to the deep level tunnel.

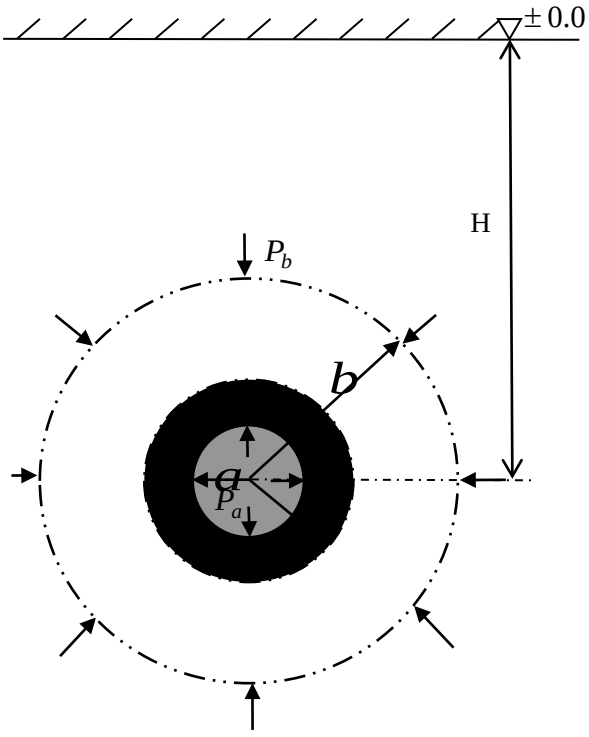

Fig.5 Circular tunnel in elastic-plastic regime

Because of the axi-symmetry of the problem, in the framework of strain gradient theory the equilibrium equation in cylindrical coordinate system (r , θ , z) may be simplified into the following form:

$$\frac{d\sigma_r^*}{dr}+\frac{1}{r}(\sigma_r^*-\sigma_\theta^*)=0 \tag{25}$$

where σ_r^* and σ_θ^* are generalized radial and tangential stresses respectively, which may be expressed as:

$$\sigma_r^*=\sigma_r-(\frac{d\tau_{rrr}}{dr}+\frac{1}{r}(\tau_{rrr}-\tau_{\theta\theta r}-\tau_{r\theta\theta})) \tag{26}$$

$$\sigma_\theta^* = \sigma_\theta - (\frac{d\tau_{\theta r\theta}}{dr} + \frac{1}{r}(\tau_{\theta r\theta} + \tau_{r\theta\theta} + \tau_{\theta\theta r}))$$ (27)

The corresponding geometrical equations are

$$\begin{cases} \varepsilon_r = \dfrac{du_r}{dr}, \varepsilon_\theta = \dfrac{u_r}{r}, \eta_{rrr} = u_{r,rr} \\ \eta_{\theta\theta r} = \dfrac{1}{r^2}(ru_{r,r} - u_r), \eta_{r\theta\theta} = \eta_{\theta r\theta} = \dfrac{1}{r}(u_{r,r} - \dfrac{u_r}{2r}) \end{cases}$$ (28)

And the boundary conditions are

$$T_a = -\sigma_r + \frac{\partial \tau_{rrr}}{\partial r} + \frac{1}{r}(-\tau_{rrr} - \tau_{\theta\theta r}) = p_a; R_a = \tau_{rrr} = 0$$ (29)

$$T_b = \sigma_r - \frac{\partial \tau_{rrr}}{\partial r} + \frac{1}{r}(-\tau_{rrr} + 2\tau_{r\theta\theta} + \tau_{\theta\theta r}) = -p_b; R_b = \tau_{rrr} = 0$$ (30)

It is assumed that the constitutive relations for the higher-order stresses remain the same in elastic and plastic regimes. Following Zhao et al. [27] we take the values of a_i as following: $a_1 = -c$, $a_2 = 7c/4$, $a_3 = -c$, $a_4 = 3c$, $a_5 = -c$, where c denotes a single gradient- dependent elastic parameter. Then constitutive equations may be written as follows：

in elastic regime： $\sigma_\theta = \lambda \dfrac{du_r}{dr} + \dfrac{\lambda + 2\mu}{r} u_r; \sigma_r = (\lambda + 2\mu)\dfrac{du_r}{dr} + \dfrac{\lambda}{r} u_r$ (31)

in plastic regime： $\sigma_\theta = k_1 \dfrac{u_r}{r} + m_1 \dfrac{du_r}{dr} + n_1; \sigma_r = k_2 \dfrac{u_r}{r} + m_2 \dfrac{du_r}{dr} + n_2$ (32)

And the higher-order stresses have the following form

$$\begin{cases} \tau_{rrr} = cl^2(5\dfrac{\partial^2 u_r}{\partial r^2} + 4\dfrac{\partial u_r}{r\partial r} - \dfrac{13}{4}\dfrac{u_r}{r^2}); \quad \tau_{r\theta\theta} = \tau_{\theta r\theta} = cl^2(\dfrac{3}{4}\dfrac{\partial^2 u_r}{\partial r^2} + \dfrac{11}{4}\dfrac{\partial u_r}{r\partial r} - \dfrac{7}{4}\dfrac{u_r}{r^2}) \\ \tau_{rzz} = \tau_{zrz} = cl^2(\dfrac{3}{4}\dfrac{\partial^2 u_r}{\partial r^2} + \dfrac{3}{4}\dfrac{\partial u_r}{r\partial r} - \dfrac{1}{2}\dfrac{u_r}{r^2}); \quad \tau_{\theta\theta r} = cl^2(\dfrac{3}{2}\dfrac{\partial^2 u_r}{\partial r^2} + \dfrac{7}{2}\dfrac{\partial u_r}{r\partial r} - \dfrac{11}{4}\dfrac{u_r}{r^2}) \\ \tau_{zzr} = cl^2(\dfrac{3}{2}\dfrac{\partial^2 u_r}{\partial r^2} + \dfrac{3}{2}\dfrac{\partial u_r}{r\partial r} - \dfrac{5}{4}\dfrac{u_r}{r^2}) \end{cases}$$ (33)

In elastic zone in terms of radial displacement u_r the equilibrium equation is obtained by substituting Eqs.(26)－(28) , (31) and (33) into Eq.(25)

$$\frac{d^4 u_r}{dr^4} - \frac{11}{5r}\frac{d^3 u_r}{dr^3} - \left[\frac{61}{20r^2} + \frac{\lambda + 2\mu}{5cl^2}\right]\frac{d^2 u_r}{dr^2} + \left[-\frac{\lambda + 2\mu}{5cl^2 r} + \frac{51}{20r^3}\right]\frac{du_r}{dr} - \left[\frac{51}{20r^4} - \frac{\lambda + 2\mu}{5cl^2 r^2}\right]u_r = 0$$ (34)

The elastic zone has the inner radius $r = \rho$ and outer radius $r = b$ respectively. At the outer surface $r = b$ the boundary conditions are

$$\begin{cases} T_b = \left\{-5cl^2\dfrac{d^3 u_r}{dr^3} - cl^2\dfrac{6}{r}\dfrac{d^2 u_r}{dr^2} + \left[\dfrac{49}{4r^2}cl^2 + (\lambda + 2\mu)\right]\dfrac{du_r}{dr} + (\dfrac{\lambda}{r} - \dfrac{19}{2r^3}cl^2)u_r + p_b\right\}_{r=b} = 0 \\ R_b = \left[5\dfrac{d^2 u_r}{dr^2} + \dfrac{4}{r}\dfrac{du_r}{dr} - \dfrac{13}{4r^2}u_r\right]_{r=b} = 0 \end{cases}$$ (35)

The boundary $r = \rho$ is the boundary between elastic and plastic zones, the medium at this boundary must satisfy equilibrium equation (25) and the following yield condition

$$\sigma_\theta^* - A\sigma_r^* = \sigma_c$$ (36)

Substituting Eq.(36) into Eq.(25) yields

$$\frac{d\sigma_r^*}{dr}+\frac{(1-A)\sigma_r^*}{r}=\frac{\sigma_c}{r} \tag{37}$$

Therefore at boundary $r=\rho$ the boundary conditions take the following form

$$\sigma_\theta^*-A\sigma_r^*=\sigma_c;\qquad \frac{d\sigma_r^*}{dr}+\frac{(1-A)\sigma_r^*}{r}=\frac{\sigma_c}{r} \tag{38}$$

Or in terms of radial displacement u_r

$$\begin{cases} cl^2\left\{(5A-\frac{3}{4})\frac{d^3u_r}{dr^3}+(\frac{27A}{4r}-\frac{23}{4r})\frac{d^2u_r}{dr^2}+\left[\frac{\lambda-A(\lambda+2\mu)}{cl^2}-\frac{18}{4r^2}-\frac{38A}{4r^2}\right]\frac{du_r}{dr}+\left[\frac{\lambda+2\mu-A\lambda}{rcl^2}+\frac{11}{4r^3}+\frac{31A}{4r^3}\right]u_r\right\}=\sigma_c \\ -5\frac{d^4u_r}{dr^4}+\frac{20(A-1)-27}{4r}\frac{d^3u_r}{dr^3}+\left[\frac{27(A-1)+65}{4r^2}+\frac{\lambda+2\mu}{cl^2}\right]\frac{d^2u_r}{dr^2}+\left[\frac{38(1-A)-107}{4r^3}+\frac{(1-A)(\lambda+2\mu)+\lambda}{r}\right]\frac{du_r}{dr} \\ +\left[\frac{31(A-1)+93}{4r^4}+\frac{\lambda(1-A)-\lambda}{r^2}\right]u_r=\frac{\sigma_c}{r} \end{cases} \tag{39}$$

In plastic zone in terms of radial displacement u_r the equilibrium equation is obtained by substituting Eqs.(26)–(28) , (32) and (33) into Eq.(25)

$$\frac{d^4u_r}{dr^4}-\frac{11}{5r}\frac{d^3u_r}{dr^3}-\left[\frac{61}{20r^2}+\frac{m_2}{5cl^2}\right]\frac{d^2u_r}{dr^2}+\left[-\frac{k_2+m_2-m_1}{5cl^2r}+\frac{51}{20r^3}\right]\frac{du_r}{dr}-\left[\frac{51}{20r^4}-\frac{k_1}{5cl^2r^2}\right]u_r-\frac{n_2-n_1}{5crl^2}=0 \tag{40}$$

The plastic zone has the inner radius $r=a$ and outer radius $r=\rho$, respectively. At the inner surface $r=a$ the boundary conditions are

$$\begin{cases} T_a=\left\{5cl^2\frac{d^3u_r}{dr^3}-cl^2\frac{5}{2r}\frac{d^2u_r}{dr^2}-\left[\frac{59}{4r^2}cl^2+m_2\right]\frac{du_r}{dr}+(-\frac{k_2}{r}+\frac{25}{2r^3}cl^2)u_r-n_2-p_a\right\}_{r=a}=0 \\ R_a=\left[5\frac{d^2u_r}{dr^2}+\frac{4}{r}\frac{du_r}{dr}-\frac{13}{4r^2}u_r\right]_{r=a}=0 \end{cases} \tag{41}$$

At the boundary $r=\rho$ between elastic and plastic zones the boundary conditions are Eq.(39).

The obtained governing equations with higher-order boundary conditions are very complex for closed-form analytical solutions; hence the numerical algorithms are used to solve these equations.

5. The numerical results and discussions

The solution of the fourth-order ordinary differential equations with two-point boundary conditions can be obtained by using ODE45 module in MATLAB software and numerical methods (Quasi-Newton method and Shooting method) [28, 29]. The following parameters for numerical analysis are taken. Tunnel radius is $a=4\,m$; the inner and outer pressure are $p_a=0$, $p_b=100MPa$, respectively; rock mass modulus is $E=20GPa$; Poisson's ratio is $\upsilon=0.20$; the friction angle is $\varphi=20.81^\circ$; the uniaxial compressive strength is $\sigma_c=50MPa$; the modulus ratio is $\xi=|M/E|=1.5$; the lateral deformation coefficient is $\beta=3.3$; the internal length scale is $l=0.04a$; the gradient-dependent elastic parameter is $c=\mu$. In the following subsections, when we study the parameter sensitivity of one of the above mentioned parameters, only the examined parameter varies with other parameters taking the above mentioned values.

Numerical calculation procedure is implemented in MATLAB software. The correctness of the algorithms and the proposed model has been verified by the authors preliminarily. The influence of model parameters,

such as υ, M, P_b/σ_c, c, l, β, on stress distribution in surrounding the tunnel rock mass is investigated in this Section.

5.1 The influence of Poisson's ratio υ

The influence of the Poisson's ratio on the mechanical behaviors of rock mass has been studied by adopting four values:, $\upsilon = 0.2$, $\upsilon = 0.3$, $\upsilon = 0.4$

Figs.6 presents the stress distribution in the plastic zone at different values of Poisson's ratio with $\rho = 10\,m$. The stress peak value envelopes are consistent with the stress distribution obtained by conventional theory. Detailed analyses show that the slope and amplitude at first monotonically decrease with the increase of Poisson's ratio, reach their minimum at $\upsilon = 0.27$, and then monotonically increase with the increase of Poisson's ratio.

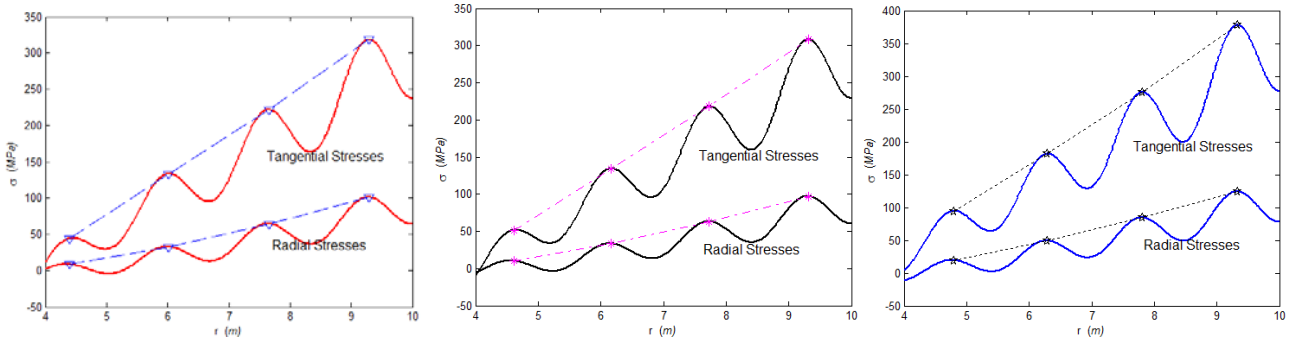

(a) (b) (c)

Fig.6 Stress distribution in surrounding tunnel rock mass under (a) $\upsilon = 0.2$, (b) $\upsilon = 0.3$ and (c) $\upsilon = 0.4$

5.2 The influence of softening modulus M

The softening modulus M is defined by the modulus ratio ξ. The stress distribution in surrounding tunnel rock mass with different values of ξ is presented in Fig.7. From Fig.7 it can be seen that when ξ is very small ($\xi = 0.1$), the constitutive relation is close to the ideal elasto-plastic model, the stress distribution in surrounding tunnel rock mass is very smooth and monotonic, and the quasi-periodic oscillating feature is very weak. With the increase of ξ, not only the oscillation and periodicity of the stress distribution become more and more remarkable, but the peak-to-trough amplitude and the absolute peak stress magnitude gradually increases, the slope of the curve becomes steeper. The obtained results indicate that softening property of rock is a controlling factor for the appearance of quasi-periodic oscillating feature of stress distribution in deep level rock mass beyond elastic limit.

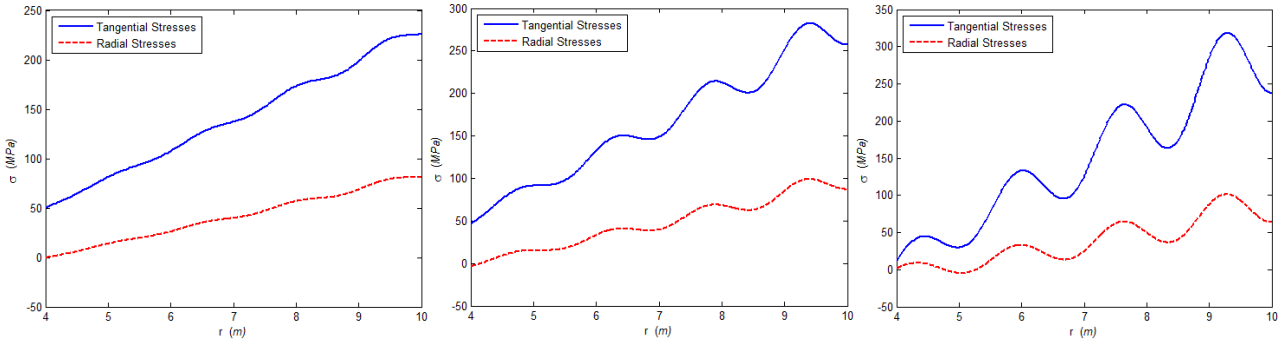

(a) (b) (c)

Fig.7 Stress distribution in surrounding tunnel rock mass under (a) $\xi = 0.1$, (b) $\xi = 0.5$ and (c) $\xi = 1.5$

5.2. The influence of internal length scale l *and the gradient-dependent elastic parameter* c

Take $\rho = 10\ m$, and keep values of other parameters unchanged, the stress distribution in surrounding tunnel rock mass can be obtained under l/a =0.021, 0.04, 0.055, respectively. The results are presented from Figs.8. It is clear that with the increase of l/a, the number of peaks and troughs decrease rapidly, the peak-to-trough amplitudes increases. Therefore internal length scale l is an important factor affecting the phenomenon of zonal disintegration**.**

To investigate the effect of gradient-dependent elastic parameter c, relevant parameters are taken: the internal length scale $l = 0.04a$, the boundary between elastic and plastic zones at $\rho = 10\ m$, and four values of c for computation: $c = 0.55\mu$, μ, 2μ. The numerical results are presented from Figs.9. It is evident that with the increase of c oscillating frequency of stress distribution decreases. When $c = 2\mu$, only three peaks and troughs occur, and the distance between two adjacent peaks increases. The influence of c is similar to that of l, so it is necessary to study their combined effect.

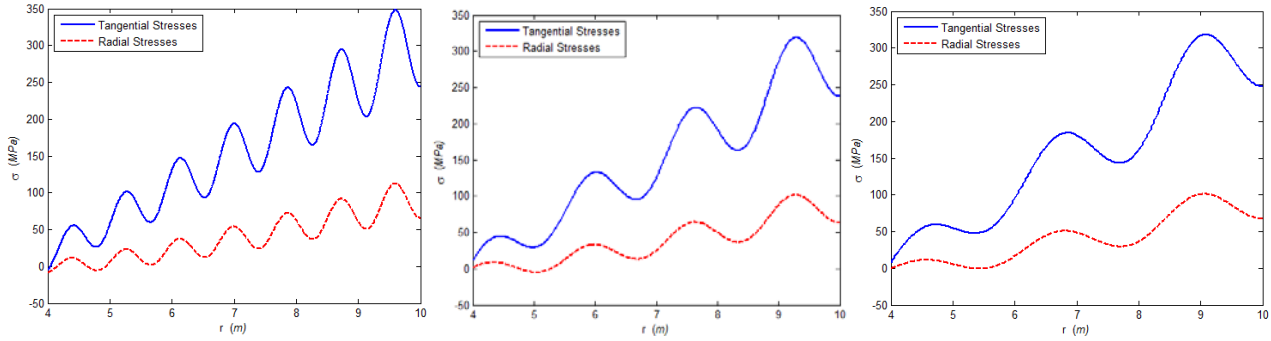

(a) (b) (c)

Fig.8 Stress distribution in surrounding tunnel rock mass under (a) $l = 0.021a$, (b) $l = 0.04a$ and (c) $l = 0.055a$

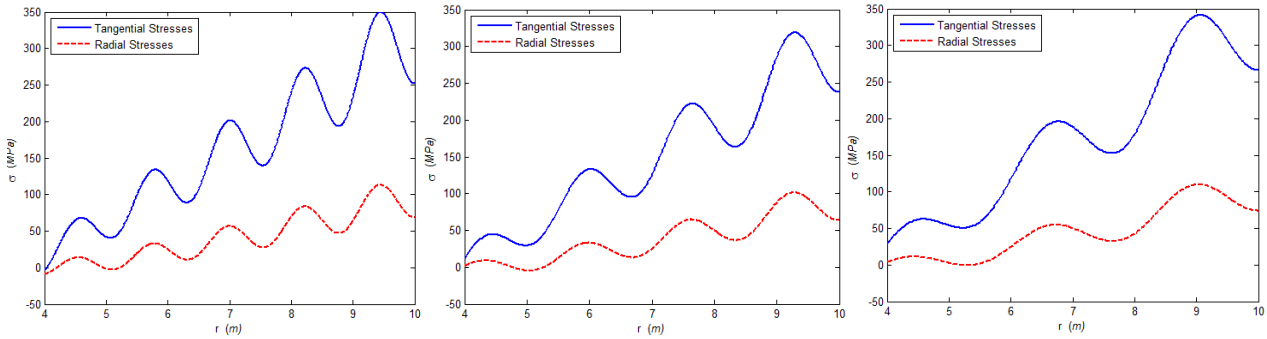

Fig.9 Stress distribution in surrounding tunnel rock mass under $c = 0.55\mu$ $c = \mu$ $c = 2\mu$

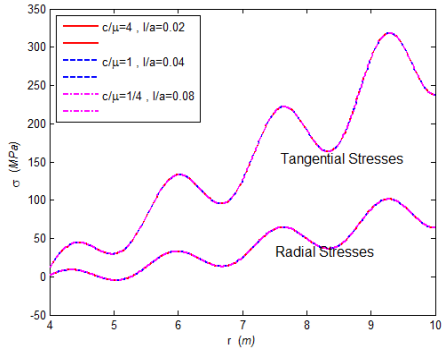

Fig.10 Stress distribution in surrounding tunnel rock mass for fixed $cl^2 = 0.0016a \cdot \mu$

Fig.10 represents the numerical results of stress distribution in surrounding tunnel rock mass obtained by taking three sets of values of c and l with fixed value of $cl^2 = 0.0016a \cdot \mu$. It is of particular interest in seeing from Fig.10 that the stress distributions in surrounding tunnel rock mass for three sets of values of c and l

coincide completely. It can then be concluded that the combination of the two parameters cl^2 is essential. Regardless of the values of c and l, if the value of cl^2 is fixed the periodicity property of the stress distribution in surrounding deep tunnel rock mass remains the same. The smaller the value of cl^2 is, the higher the oscillating frequency of the stress distribution in surrounding deep tunnel rock mass is.

5.3 The influence of lateral deformation coefficient

Figs.11 present the stress distribution in surrounding tunnel rock mass for four values of lateral deformation coefficient $\beta = 2.5, 5.0, 10.0$.

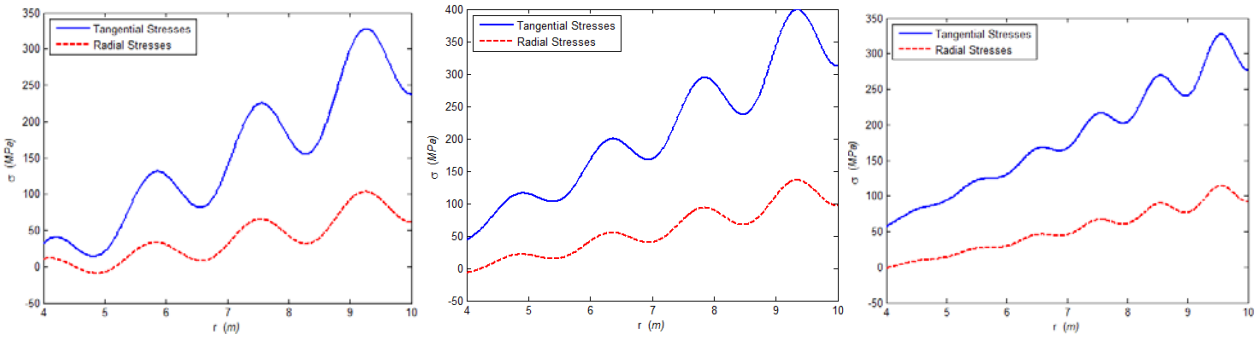

(a) (b) (c)

Fig.11 Stress distribution in surrounding tunnel rock mass at (a) $\beta = 2.5$, (b) $\beta = 5.0$, (c) $\beta = 10.0$

The numerical results from Figs.11 show that with the increase of β the oscillating feature of stress distribution becomes weaker and weaker, but the oscillating frequency of stress distribution curves increases.

5.4 The influence of relative loading level $\overline{\sigma} = P_b/\sigma_c$

The following parameters for numerical analysis of stress field in surrounding tunnel rock mass are taken. Tunnel radius is $a = 4\ m$; the inner pressure are $p_a = 0$; rock mass modulus is $E = 20GPa$; rock mass's Poisson's ratio is $\upsilon = 0.20$; the friction angle is $\varphi = 20.81^\circ$; the uniaxial compressive strength is $\sigma_c = 50MPa$; the modulus ratio is $\xi = |M/E| = 1.5$; the lateral deformation coefficient is $\beta = 3.3$; the gradient-dependent elastic parameter is $c = \mu$; the internal length scale is taken as $l = 0.04a$ by data fitting to the experimental data.

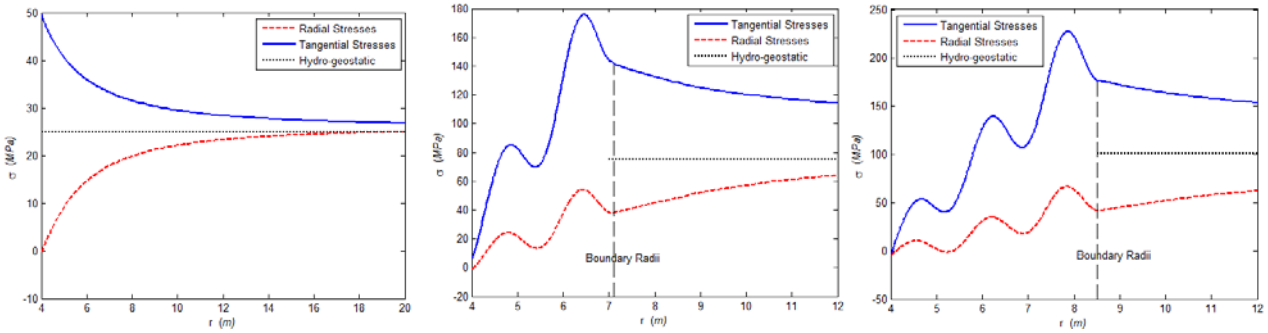

(a) (b) (c)

Fig.12 Stress distribution in surrounding tunnel rock mass when (a) $\overline{\sigma} = 0.5$, (b) $\overline{\sigma} = 1.5$, (c) $\overline{\sigma} = 2.0$

When $\overline{\sigma} = P_b/\sigma_c = 0.5$ the inner surface of tunnel begins to yield as the stresses at $r = a$ satisfy the Mohr-Coulomb's criterion. The stress distribution in surrounding tunnel rock mass is presented in Fig.12(a). Figs.12(b) and (c) give the stress fields in surrounding tunnel rock mass obtained at $\overline{\sigma} = 1.5$ and $\overline{\sigma} = 2.0$, respectively. Fig.12(b) shows that when $\overline{\sigma} = 1.5$ the boundary between elastic and plastic zones is at $r = 7.10\ m$, and there are

two peaks and troughs. There are three peaks and troughs when $\overline{\sigma} = 2.0$, as shown in Fig.12(c). The numerical results are in agreement with the experimental results [3]. Meanwhile the boundary between elastic and plastic zones when $\overline{\sigma} = 2.0$ is at $r = 8.55\,m$, farther than that in the case of $\overline{\sigma} = 1.5$. Therefore it can be concluded that the number of fractured zones will increase with the increase of the tunnel depth. When relative loading level is about 0.5, rock mass near tunnel surface will begin to yield first. Only when $\overline{\sigma}$ reaches a definite value, in other words, only when the depth of tunnel reaches definite value, the phenomenon of zone disintegration may occur.

6. Discussion and summary

The main results of numerical analysis of the developed in this paper gradient model are given as follows:

(1) High initial hydro-geostatic pressure is a necessary condition for the formation of zonal disintegration. Under high enough initial hydro-geostatic pressure, surrounding tunnel rock mass reaches plastic regime, which develops condition for the occurrence of dissipative structures.

(2) Softening is another necessary condition for the formation of zonal disintegration. With the increase of softening modulus, not only the oscillation and periodicity of the stress distribution become more and more notable, but the peak-to-trough amplitude and the slope of the stress distribution envelop increase.

(3) Internal length scale l and gradient-dependent elastic parameter c have similar effect on zonal disintegration. In general, with the increase of l and c the number of peaks and troughs decreases rapidly, while the peak-to-trough amplitudes increases. The combination of the two parameters cl^2 reflects the gradient nature of materials. If the value of cl^2 is fixed, no matter what values c and l are taken, the periodicity property of the stress distribution in surrounding deep tunnel rock mass remains the same. The smaller the value of cl^2 is, the higher the oscillating frequency of the stress distribution is. cl^2 is the third parameter controlling the oscillation and periodicity feature of the stress distribution.

(4) With the increase of lateral deformation coefficient β the oscillating feature of stress distribution curves becomes weaker and weaker, but the oscillating frequency of stress distribution curves increases. Therefore this parameter is also a parameter affecting the quasi-periodic variation of stress distribution in deep level rock mass.

(5) Poisson's ratio υ mainly affects on the slope and the amplitude of stress peak value envelopes. The slope and amplitude of stress distribution monotonically decrease at the beginning with the increase of υ, and reach their minimum at $\upsilon = 0.27$, then monotonically increase with the increase of Poisson's ratio.

ACKNOWLEDGEMENT

The study was conducted with financial support of the National Natural Science Foundation of China (NSFC grants No 51478027, 51174012), the "973" Key State Research Program (grant No. 2015CB0578005), Science Fund for Creative Research Groups of the National Natural Science Foundation of China (NSFC grant No. 51021001).

References

1. Shemykin E.I., Fisenko G.N., Kurlenja M.V. et al. The rock-mass zone disintegration near deep level mining opening. Part I: Data of in situ observations. J Min Sci 1986; 22(3): 3-13.
2. Tan Y.L., Ning J.G., Li H.T., In situ explorations on zonal disintegration of roof strata in deep coalmines. Int J Rock Mech Min Sci 2012; 49:113–124.
3. Shemykin E.I., Fisenko G.N., Kurlenja M.V. et al. The rock-mass zone disintegration near deep level mining opening. Part II: The fracture of rock in models from equivalent materials. J Min Sci 1986; 22(4): 3-15.
4. Shemykin E.I., Fisenko G.N., Kurlenja M.V. et al. The rock-mass zone disintegration near deep level mining opening. Part III: Theoretical repesentation. J Min Sci 1987 ; 23(1): 3-8.
5. Shemykin E.I., Fisenko G.N., Kurlenja M.V. et al. The rock-mass zone disintegration near deep level mining opening. Part IV: Practical application. J Min Sci 1989; 25(4): 3-9.
6. Kurlenja M.V., Oparin V.N., Bobrov G.F.et al. On splitting effect in zones of supporting pressure. J Min Sci 1995; 31(5): 3-11.
7. Gu J.C., Gu L.Y., Chen A.M. Model test study on mechanism of layered fracture within surrounding rock of tunnels in deep

stratum. Chinese Journal of Rock Mechanics and Engineering, 2008; 27(5): 433-4384.
8. Zhang Q.Y., Chen X.G., Lin B. et al. Study of 3D geomechanical model test of zonal disintegration of surrounding rock of deep tunnel. Chinese Journal of Rock Mechanics and Engineering, 2009; 28(9)： 1757-1766.
9. Chanyshev A.I. On problem of fracture of deformable media. Part I: Basic equations. J Min Sci 2001; 37(2): 273-288.
10. Chanyshev A.I. On problem of fracture of deformable media. Part. II: Discussion of results of analytical solutions. J Min Sci 2001; 37(3): 392-400.
11. Gusev M.A., Paroshin A.A. Non-Euclidian model of rock-mass zone disintegration near underground mining opening, Appl Mech Tech Phys 2001; 42(1):147-156.
12. Jirasek M., Rolshoven S. Localization properties of strain softening gradient plasticity. Part I: strain gradient theories. Int J Solids Struct 2009, 46:2225-2238.
13. Jirasek M., Rolshoven S. Localization properties of strain softening gradient plasticity. Part II: Theories with gradients of internal variables. Int J Solids Struct 2009, 46:2239-2254.
14. Toupin R.A. Elastic materials with couple stresses. Arch Ration Mech Anal 1962; 11(1) :385–414.
15. Mindlin R.D. Second gradient of strain and surface tension in linear elasticity. Int J Solids Struct 1965; 28: 845–857.
16. Eshel N., Rosenfeld G. Axi-symmetric problems in elastic materials of grade two. J Franklin Inst 1975; 299(1): 43–51.
17. Fleck N.A., Hutchinson J.W. Strain gradient plasticity. In: Hutchinson, J.W., Wu, T.Y. (Eds.), Advances in Applied Mechanics, 1997; 33:295-361, Academic Press, New York.
18. M.E.Gurtin, A gradient theory of single crystal visco-plasticity that accounts for geometrically necessary dislocations. J Mech Phys Solids 2002; 50: 5-32.
19. Aifantis E.C. On the Microstructural Origin of Certain Inelastic Models. J Eng Mater Tech 1984; 106:326-330.
20. Aifantis E.C. Pattern formation in plasticity. Int J Eng Sci 1995; 33:2161-2178.
21. Polizzotto C. Unified thermodynamic framework for nonlocal/gradient continuum theories. Eur J Mech A: Solids 2003; 17(3) : 651- 668.
22. Abu Al-Rub R.K., Voyiadjis G.Z. and Bammann J.B. A thermodynamic based higher-order gradient theory for size dependent plasticity. Int J Solids Struct 2007; 44: 2888-2923.
23. Fleck N.A. and Willis J.R. A mathematical basis for strain-gradient plasticity theory. Part II: tensorial plastic multiplier. J Mech Phys Solids 2009; 57:1045–1057.
24. Wang M.Y., Qi C.Z., Qian Q.H. and Chen J.J., 2012. One plastic gradient model of zonal disintegration of rock mass near deep level tunnels. J Min Sci 2012; 48(1) :54-62
25. Ilyjushin A.A. Plasticity. OGIZ, Moscow-Leningrad, 1948.
26. Baklashov I.V., Kartozia B.A. Mechanics of underground buildings and structures. Nedra, Moscow, 1984.
27. Zhao J.D., Sheng D.C. and Sloan S.W. Cavity expansion of a gradient-dependent solid cylinder. Int J Solids Struct 2007; 44: 4342-4368.
28. Keller H.B., Numerical methods for two-point boundary-value problems, Blaisdell Pub. Co., Waltham, MA, London, 1968.
29. Chambon R., Moullet J.C., Uniqueness studies in boundary value problems involving some second gradient models, Comp. Methods Appl Mech Eng 2004, 193:2771-2796.